

STABLE AND EFFICIENT SHIFT-VARIANT ALGORITHM FOR CIRCLE-PLUS-LINES ORBITS IN CONE-BEAM C.T.

F. Noo

University of Liège, Belgium
noo@montefiore.ulg.ac.be

R. Clack

University of Utah, U.S.A.
rolf@doug.med.utah.edu

M. Defrise

Free University of Brussels, Belgium
michel@vub.vub.ac.be

T. J. Roney, T. A. White, S. G. Galbraith

Idaho National Engineering Laboratory, U.S.A.
tiy@inel.gov

ABSTRACT

Defrise and Clack, and also Kudo and Saito, have derived an exact algorithm suited to accurately reconstruct cone-beam data acquired from any complete orbit. These algorithms are written in the form of a shift-variant filtered backprojection. Their main characteristic is their capability to handle in many different ways the redundancy inherent to cone-beam data sets. In this paper, we investigate the interplay between the redundancy handling and the stability and efficiency of the algorithm. Specifically, we show how to handle the redundancy to turn shift-variant filtering of some projections into shift-invariant filtering. Invoking this result, we define then a new algorithm suited to accurately and efficiently reconstruct data acquired from circle-plus-lines orbits. The new algorithm is tested on simulated data and real data from industrial imaging of waste containers.

1. INTRODUCTION

The problem of reconstructing a 3D image from its line integrals can be formulated in many different ways depending on the data acquisition process. In this paper, the studied object is of finite extent and the data are collected as cone-beam (CB) projections. A CB projection is a set of line integrals diverging from a vertex point. A CB data acquisition consists of measuring CB projections for all the vertex points lying on a specified trajectory surrounding the object. This trajectory is usually called the orbit although it is not necessarily circular, closed or even connected. For exact reconstruction, the orbit must satisfy Tuy's completeness condition [1], i.e. a plane passing through the object must also intersect the orbit.

Cone-beam computed tomography is currently used in medical and industrial imaging. Usually, the orbit is taken as a single circle and the data are reconstructed using a filtered backprojection (FBP) algorithm [2], denoted as FDK. This algorithm is stable and efficient but yields approximate reconstructions due to the incompleteness of the orbit.

The development of practical algorithms which provide theoretically exact reconstruction began only in 1987 with the work of Grangeat [3]. This author derived a mathematical relationship which links the CB data to the 3D Radon transform of the object, and subsequently proposed a reconstruction algorithm based on this result. Invoking Grangeat's formula, Defrise and Clack [4], and independently Kudo and Saito [5], have derived exact shift-variant FBP algorithms suited to process any complete set of data. These algorithms however, reconstruct the CB projections less efficiently than FDK and are more sensitive to discretization errors. Considering orbits consisting of one circle plus some lines [6], designed to satisfy Tuy's condition, Kudo and Saito have recently proposed a Hybrid algorithm [7] which reconstructs the circle data using FDK and the line data using the shift-variant FBP algorithm.

Cone-beam data acquired from complete orbits are usually redundant in the sense that any plane crossing the object contains a variable number of vertex points. The cornerstone of the FBP algorithms [4], [5], [7] is their capability to handle this redundancy in many different ways. The purpose of this communication is to investigate more deeply this property for the Defrise-Clack (DC) algorithm so as to define a stable and efficient shift-variant FBP algorithm for circle-plus-lines orbits. The new algorithm is tested on simulated data and on real data acquired from an experimental 3D X-ray scanner, designed for industrial imaging of waste containers [8].

2. THE DC-FBP ALGORITHM

The orbit trajectory is parameterized by the scalar λ with each vertex point $\underline{a}(\lambda)$ assumed to lie on the surface of an imaginary cylinder centered around the z -axis of the fixed reference frame. Mathematically, cone-beam projections are measured for each λ in the one-dimensional set Λ , but in practice a finite number of vertex points are sampled from Λ at some spacing $\Delta\lambda$. The detector, also parameterized by λ , is oriented such that it is parallel to the plane tangent to the cylinder at the vertex point $\underline{a}(\lambda)$. The λ -detector is always a distance D from its corresponding vertex point $\underline{a}(\lambda)$.

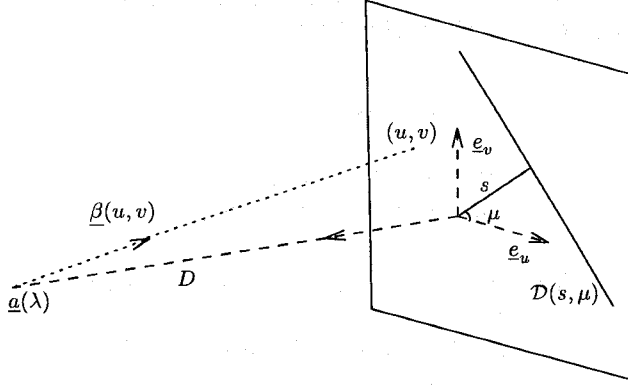


Figure 1: Acquisition geometry

Locations (u, v) on the detector are coordinates taken with respect to the vectors \underline{e}_u and \underline{e}_v which are respectively horizontal (parallel to the plane $z = 0$) and vertical (parallel to the z -axis). The object to be reconstructed is denoted $f(\underline{x})$ and always lies between the vertex point and the detector.

The vertex point $\underline{a}(\lambda)$ and the coordinates (u, v) on the λ -detector define a line of direction $\underline{\beta}(u, v)$ along which the line integral $g(u, v, \lambda)$ is measured (see fig. 1) :

$$g(u, v, \lambda) = \int_0^\infty dt f(\underline{a}(\lambda) + t \underline{\beta}(u, v)) \quad (1)$$

The detector is assumed to be large enough so that all lines diverging from $\underline{a}(\lambda)$ which pass through the object f are measured.

The DC-FBP algorithm [4] reconstructs the image f from its projections g in three steps. The first and third steps are identical to those of the FDK algorithm. The steps described below are a slightly simplified version of those in [4], and apply specifically to the orbit and detector geometry described above.

Step 1 : Pre-scaling. The scaled CB projections are

$$g_\omega(u, v, \lambda) = \frac{D}{\sqrt{u^2 + v^2 + D^2}} g(u, v, \lambda) \quad (2)$$

Step 2 : Shift-variant filtering. The filtered CB projections are computed as the 2D backprojection

$$g_F(u, v, \lambda) = \int_0^\pi d\mu k(u \cos \mu + v \sin \mu, \mu, \lambda) \quad (3)$$

of the sinogram function

$$k(s, \mu, \lambda) = -\frac{|\underline{a}'(\lambda)|}{4\pi^2 D} \left\{ |\cos(\mu - \phi_\lambda)| M(s, \mu, \lambda) \left(\frac{\partial}{\partial s} \mathcal{R}g_\omega \right) (s, \mu, \lambda) \right\} \quad (4)$$

defined on the λ -detector. A pair (s, μ) specifies a line $\mathcal{D}(s, \mu)$ in the detector (see fig. 1) and $(\mathcal{R}g_\omega)(s, \mu, \lambda)$ is the integral of $g_\omega(u, v, \lambda)$ along this line. The angle between the vector $\underline{a}'(\lambda)$ tangent to the orbit and the horizontal plane

is ϕ_λ . In practice, the term $|\underline{a}'(\lambda)|$ represents the distance between consecutive vertex points. The function $M(s, \mu, \lambda)$ is discussed below.

Step 3 : CB backprojection. The value of the image f at point \underline{x} is

$$f(\underline{x}) = \int_\Lambda d\lambda \frac{u^2 + v^2 + D^2}{|\underline{x} - \underline{a}(\lambda)|^2} g_F(u, v, \lambda) \quad (5)$$

where, for λ fixed, (u, v) is the intersection between the detector and the line connecting \underline{x} to the vertex point.

The weighting function $M(s, \mu, \lambda)$ handles redundancy in the cone-beam data. The significance of M at a point $(s_\alpha, \mu_\alpha, \lambda_\alpha)$ can be explained as follows. The line $\mathcal{D}(s_\alpha, \mu_\alpha)$ and the vertex point $\underline{a}(\lambda_\alpha)$ define a plane Π . This plane intersects the orbit at $n(\Pi)$ vertex points

$$\underline{a}(\lambda_\alpha), \alpha = 0, \dots, n(\Pi) - 1$$

with lines $\mathcal{D}(s_\alpha, \mu_\alpha)$ on associated λ_α -detectors. The points $(s_\alpha, \mu_\alpha, \lambda_\alpha)$ give identical contributions to the image and must therefore be given a relative weight $M(s_\alpha, \mu_\alpha, \lambda_\alpha)$ so that the total contribution is unity:

$$\sum_{\alpha=0}^{n(\Pi)-1} M(s_\alpha, \mu_\alpha, \lambda_\alpha) = 1 \quad (6)$$

The easiest way to satisfy equation (6) is to take

$$M(s_\alpha, \mu_\alpha, \lambda_\alpha) = 1/n(\Pi)$$

which means the plane Π is given the same weight for each of the vertex points that it contains. Such a choice however, leads to a discontinuous weighting function and makes the outer derivative step in equation (4) numerically unstable. A differentiable solution for M can be found in [4].

3. EFFICIENT WEIGHTING FUNCTION

The shift-variant filtering of a CB projection (step 2) in the DC-FBP algorithm requires a sinogram (set of line integrals) to be computed, and requires a 2D backprojection operation. These tasks, although they can be implemented using linogram techniques [9], are computationally intensive. However, if the factor $M(s, \mu, \lambda)$ were not present in equation (4), then equations (3) and (4) would mathematically collapse to a much simpler and more efficient operation. We show here that this simplification still occurs if the function M is independent of s . Specifically, we show that if $M = M(\mu, \lambda)$, then g_ω and g_F are related by a simple 2D convolution.

For M independent of s the RHS of equation (4) simplifies and, using the central section theorem, the Fourier transform of $k(s, \mu, \lambda)$ is calculated as

$$(\mathcal{F}_1 k)(\sigma, \mu, \lambda) = \frac{|\underline{a}'(\lambda)|}{D} |\cos(\mu - \phi_\lambda)| M(\mu, \lambda) \sigma^2 (\mathcal{F}_2 g_\omega)(\sigma \cos \mu, \sigma \sin \mu, \lambda) \quad (7)$$

where \mathcal{F}_1 and \mathcal{F}_2 denote the 1D and 2D Fourier transforms. Combining this result with equation (3) yields

$$(\mathcal{F}_2 g_F)(k_u, k_v, \lambda) = H_\lambda(k_u, k_v) (\mathcal{F}_2 g_\omega)(k_u, k_v, \lambda) \quad (8)$$

where

$$H_\lambda(k_u, k_v) = \frac{|a'(\lambda)|}{D} |k_u \cos \phi_\lambda + k_v \sin \phi_\lambda| M(\mu, \lambda)$$

and the angle μ is given by $\tan \mu = k_v/k_u$. That is, g_ω and g_F are linked by the 2D filter $H_\lambda(k_u, k_v)$ and step 2 can be very efficiently implemented using 2D FFT.

4. CIRCLE-PLUS-LINES ORBITS

An orbit consisting of one circle \mathcal{C} in the horizontal plane $z = 0$ and of $N \geq 1$ vertical lines located at some positions on the circle [6], satisfies Tuy's condition provided the height of the lines is adequately chosen. Processing this orbit with the DC-FBP algorithm and the usual M function [4] is relatively inefficient because of the shift-variant filtering of step 2.

An efficient algorithm for circle-plus-lines orbits would be achieved if the filter applied to most of the projections were shift-invariant. Invoking the results of section 3, we have defined a weighting function M which satisfies equation (6), yields a shift-invariant filter on the circle, and can be differentiated for stable processing of the line data. This function M yields filtering steps as follows. For projections whose vertex point lies on the circle, step 2 is given by equation (8) with

$$M(\mu, \lambda) = \begin{cases} \frac{1}{2} \left(1 - \exp\left(\frac{\cos^2 \mu}{\cos^2 \mu - \sin^2 \mu_0}\right) \right) & \text{if } |\cos \mu| \leq \sin \mu_0 \\ \frac{1}{2} & \text{otherwise} \end{cases} \quad (9)$$

where μ_0 is a small fixed angle and the region

$$|\cos \mu| \leq \sin \mu_0$$

corresponds to planes which are nearly tangent to the circle. For vertex points on any of the lines, the shift-variant filtering of equations (3) and (4) is used with

$$M(s, \mu, \lambda) = \begin{cases} M_{\mathcal{L}}(s, \mu, \lambda) & \text{if } \Pi(s, \mu, \lambda) \cap \mathcal{C} = \emptyset \\ M_{\mathcal{L}}(s, \mu, \lambda) (1 - 2M(\mu_c, \lambda_c)) & \text{otherwise} \end{cases} \quad (10)$$

where $\lambda_c \in \mathcal{C}$ is a vertex point on the circle and in the plane $\Pi(s, \mu, \lambda)$, and μ_c is the angle of the line of intersection of $\Pi(s, \mu, \lambda)$ with the λ_c -detector. The function $M_{\mathcal{L}}(s, \mu, \lambda)$ was computed using the differentiable solution [4] to equation (6) for an orbit consisting of the N lines only.

To summarize, the new algorithm reconstructs the circle data using the shift-invariant filter (equations (8) and (9)) and the line data using the shift-variant filter (equations (3), (4) and (10)). The pre-scaling and CB backprojection steps, equations (2) and (5), are similar for the circle data and the line data.

The algorithm proposed here reduces to the Hybrid approach of Kudo and Saito [7] as μ_0 tends to zero, but in this case the M function for the line data is no longer differentiable.

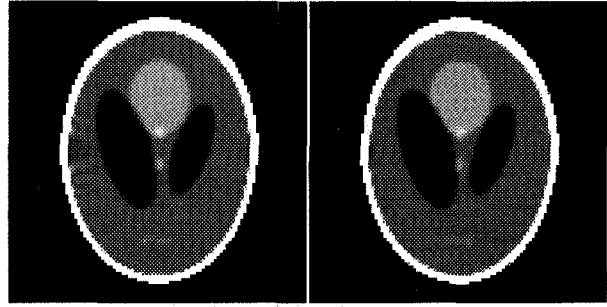


Figure 2: Slice $y = -124\text{mm}$ through the 3D Shepp phantom, reconstructed using (a) DC-FBP (b) New algorithm

5. RECONSTRUCTIONS

5.1. Simulated data

The classical 3D Shepp phantom was used to demonstrate the accuracy of the algorithm for reconstructing low contrast objects. The orbit was one circle (120 vertex points) and three lines (20 vertex points on each) equiangularly spaced. The detector consisted of 128×128 square pixels of side 2.5mm. The source was a distance 400mm from the z axis and a distance $D = 590\text{mm}$ from the detector. The data were reconstructed on a grid of 100^3 cubic voxels of side 2mm, and displayed using a compressed greyscale to illustrate the 1% to 2% contrast differences inside the phantom. Figure 2 shows that the phantom was as accurately reconstructed as with DC-FBP, with artefacts only appearing at the 0.5% level.

The reconstruction cpu times on a Sun Ultra Sparcstation (167MHz) are given in the table below. Filtering times depends only on projection data dimensions, and backprojection time only on number of reconstructed voxels. The total times were 761s cpu time for DC-FBP, and 403s cpu time for the new algorithm.

cpu time/ projection	filtering on circle	filtering on line	backpr.
DC-FBP	3.29s	3.29s	0.94s
New Algorithm	0.30s	3.29s	0.94s

5.2. Real data

Real CB data was collected on a large x-ray scanner designed for imaging 55 gallon drums (radius 300mm, height 880mm) of radioactive waste. X-rays were generated with a 420kVp source and the detector surface consisted of a $105 \times 127.5\text{mm}$ Gadolinium Oxysulfide phosphor screen, lens-coupled to a 12-bit CCD camera, so that effective detector pixel size was 1.08mm square. The drum platform could rotate and the source could be moved vertically. The test drum contained vertically segmented layers of graphite and three tall vertical cylinders used for holding surrogate radiation sources. A circle-plus-3-lines scan was performed with 180 vertex points on the circle and 19 on each of the 3 lines. The source was a distance 1740mm from the rotation axis and a distance $D = 2337\text{mm}$ from the detector.

The projection data, slightly truncated in the vertical direction (fig. 3a), were compressed onto grids of 192×255

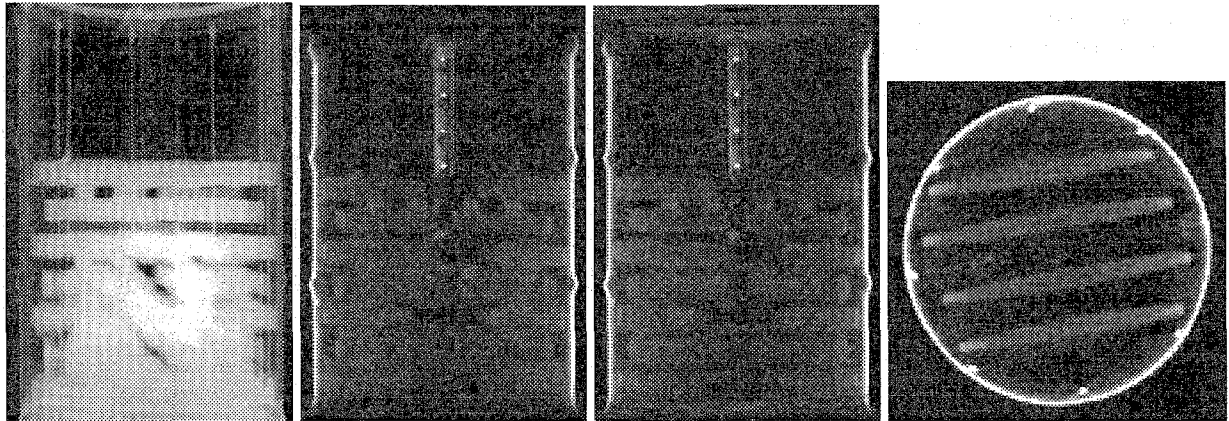


Figure 3: Industrial CT data : (a) circle projection, (b) FDK algorithm, slice $x = 0\text{mm}$, (c) new algorithm, slice $x=0\text{mm}$, (d) new algorithm $z = 25\text{mm}$, enlarged 22% with respect to fig. 3c. The x - y - z reference frame is centered in the drum.

square pixels of side 4.32mm. The data were reconstructed on a grid of $124 \times 124 \times 200$ cubic voxels of side 5mm. Figure 3a shows a CB projection of the drum for a vertex point lying on the circle. Figures 3b and 3c show a central vertical slice reconstructed using FDK (circle data only), and using the new algorithm. Some minor artefacts appear near the top and bottom of these images due to the vertical truncation evident in figure 3a. The poor recovery of the graphite layers below the middle of the drum in the FDK image (fig. 3b) illustrates the effects of the incomplete circle-only orbit. Figure 3d shows a horizontal slice reconstructed with the new algorithm, showing the four bars used to separate the top two graphite layers. Cross sections of the three vertical cylinders are also visible.

The reconstruction times on a Sun Sparcstation 20 (75 MHz) were 938s cpu time for FDK and 3589s for the new algorithm. The breakdown is given in the table below. The cpu times needed for filtering a non-compressed 700×1024 projection are 26s for FDK and, 144s and 850s for the shift-invariant and shift-variant filters of the new algorithm.

cpu time/ projection	filtering on circle	filtering on line	backpr.
FDK	0.51s		4.70s
New Algorithm	2.68s	34.96s	4.70s

6. CONCLUSIONS

A new exact shift-variant FBP algorithm for circle-plus-lines orbits has been derived. The derivation is based on a new result which clarifies the link between filtering and redundancy handling. The algorithm, tested on both simulated and real data is stable and efficient.

7. ACKNOWLEDGEMENT

Frédéric Noo is a Research Assistant and Michel Defrise is a Senior Researcher, both supported by the Belgian National fund for Scientific Research. This work was partially supported by a grant from the Whitaker Foundation, U.S.A.

8. REFERENCES

- [1] H. K. Tuy, "An inversion formula for cone-beam reconstruction," *SIAM J. Appl. Math.*, 43, 546-552, 1983.
- [2] L. A. Feldkamp, L. C. Davis, J. W. Kress, "Practical cone-beam algorithm," *J. Opt. Soc. Am.*, A6, 612-619, 1984.
- [3] P. Grangeat, *Analyse d'un système d'imagerie 3D par reconstruction à partir de radiographies X en géométrie conique*, Ph.D. Thesis, Ecole Nationale Supérieure des Télécommunications, France, 1987.
- [4] M. Defrise, R. Clack, "A cone-beam reconstruction algorithm using shift variant filtering and cone-beam backprojection," *IEEE Trans. Med. Imag.*, 13, 186-195, 1994.
- [5] H. Kudo, T. Saito, "Derivation and implementation of a cone-beam reconstruction algorithm for nonplanar orbits," *IEEE Trans. Med. Imag.*, 13, 196-211, 1994.
- [6] G. L. Zeng, G. T. Gullberg, "A cone-beam algorithm for orthogonal circle-and-line orbit," *Phys. Med. Biol.*, 37, 563-578, 1992.
- [7] H. Kudo, T. Saito, "An extended completeness condition for exact cone-beam reconstruction and its application," *IEEE Conference Record of the 1994 Nuclear Science Symposium and Medical Imaging Conference*, Norfolk, VA., 1995.
- [8] T. J. Roney, S. G. Galbraith, T. A. White, M. O'Reilly, R. Clack, M. Defrise, F. Noo, "Feasibility and Applications of Cone Beam X-Ray Imaging for Containerized Waste," *Proceedings for the 4th Nondestructive Assay and Nondestructive Examination Waste Characterization Conference*, Salt Lake City, pp. 295-324, 1995.
- [9] C. Axelsson-Jacobson, M. Defrise, P. E. Danielsson, R. Clack, F. Noo, "Exact 3D-reconstruction using cone-beam backprojection, the Radon transform and linogram techniques," *IEEE Conference Record of the 1995 Nuclear Science Symposium and Medical Imaging Conference*, San Francisco, CA, 1996.